17. Chyba, C. & Sagan, C. Electrical energy sources for organic synthesis on the early Earth. *Origins Life Evol. Biosph.* **21**, 3–17 (1991).

18. Rye, R., Kuo, P. H. & Holland, H. D. Atmospheric carbon dioxide concentrations before 2.2 billion years ago. *Nature* **378**, 603–605 (1995).

19. Zahnle, K. J. Photochemistry of methane and the formation of hydrocyanic acid (HCN) in the Earth's early atmosphere. *J. Geophys. Res.* **91**, 2819–2834 (1986).

20. Pavlov, A. A., Kasting, J. K., Brown, L. L., Rages, K. A. & Freedman, R. Greenhouse warming by CH_4 in the atmosphere of early Earth. *J. Geophys. Res.* **105**, 11981–11990 (2000).

21. Kasting, J. F., Pavlov, A. A. & Siefert, J. L. A coupled ecosystem-climate model for predicting the methane concentration in the Archean atmosphere. *Origins Life Evol. Biosph.* **31**, 271–285 (2001).

22. Yung, Y. L., Allen, M. & Pinto, J. P. Photochemistry of the atmosphere of Titan. *Astrophys. J. Suppl. Ser.* **203**, 465–506 (1984).

23. Young, J. P. W. in *Biological Nitrogen Fixation* (eds Stacey, G., Burris, R. H. & Evans, H. J.) 43–86 (Chapman & Hall, New York, 1992).

24. Beaumont, V. & Robert, F. Nitrogen isotope ratios of kerogens in Precambrian cherts: a record of the evolution of atmospheric chemistry? *Precambrian Res.* **96**, 63–82 (1999).

25. Rye, R. & Holland, H. D. Paleosols and the evolution of atmospheric oxygen: a critical review. *Am. J. Sci.* **298**, 621–672 (1998).

26. Golubic, S., Sergeev, V. N. & Knoll, A. H. Mesoproterozoic *Archaeoellipsoides*: akinetes of heterocystous cyanobacteria. *Lethaia* **28**, 285–298 (1995).

27. Brocks, J. J., Logan, G. A., Buick, R. & Summons, R. Archean molecular fossils and the early rise of eukaryotes. *Science* **285**, 1033–1036 (1999).

28. Schopf, J. W. & Parker, B. M. Early Archean (3.3-billion to 3.5-billion-year-old) microfossils from Warrawoona Group, Australia. *Science* **237**, 70–73 (1987).

29. Schopf, J. W. in *Prokaryotic Development* (eds Brun, Y. V. & Shimkets, L. J.) 105–129 (American Society of Microbiology, Washington DC, 2000).

30. Jebens, D. S., Lakkaraju, H. S., McKay, C. P. & Borucki, W. J. Time resolved simulation of lightning by LIP. *Geophys. Res. Lett.* **19**, 273–276 (1992).

....

Annual monsoon rains recorded by Jurassic dunes

David B. Loope*, Clinton M. Rowe* & R. Matthew Joeckel†

* *Department of Geosciences, University of Nebraska, Lincoln, Nebraska 68588-0340, USA*
† *Conservation & Survey Division, University of Nebraska, Lincoln, Nebraska 68588-0517, USA*

....

Pangaea, the largest landmass in the Earth's history, was nearly bisected by the Equator during the late Palaeozoic and early Mesozoic eras. Modelling experiments and stratigraphic studies have suggested that the supercontinent generated a monsoonal atmospheric circulation that led to extreme seasonality[1-3], but direct evidence for annual rainfall periodicity has been lacking[4]. In the Mesozoic era, about 190 million years ago, thick deposits of wind-blown sand accumulated in dunes of a vast, low-latitude desert at Pangaea's western margin[5-7]. These deposits are now situated in the southwestern USA. Here we analyse slump masses in the annual depositional cycles within these deposits, which have been described for some outcrops of the Navajo Sandstone[8]. Twenty-four slumps, which were generated by heavy rainfall, appear within one interval representing 36 years of dune migration. We interpret the positions of 20 of these masses to indicate slumping during summer monsoon rains, with the other four having been the result of winter storms. The slumped lee faces of these Jurassic dunes therefore represent a prehistoric record of yearly rain events.

In the southwestern United States, wind-deposited sands accumulated to a thickness of 2,500 m during the 160 million years when Pangaea straddled the Equator[6-8] (Fig. 1). These strata are the thickest and most widespread aeolian dune deposits known from the global sedimentary record. Aeolian sedimentation near the western margin of Pangaea began soon after its assembly in the Late Carboniferous period, and continued until the breakup of the supercontinent in the Late Jurassic period. The Lower Jurassic Navajo Sandstone is the thickest unit in this sedimentary succession, reaching a thickness of 700 m in southwestern Utah (17° N palaeolatitude). Most of the Navajo Sandstone consists of thick cross-strata produced by the migration and climb of large desert dunes. The dominant winds in the area during the Triassic and Early Jurassic periods were northwesterly, whereas northeasterly flow dominated during deposition of the Middle Jurassic Entrada Sandstone[7].

Other workers have recognized depositional cycles within the Navajo Sandstone that record an annual shift in wind direction[8]. These cycles consist of: (1) packages of 20–50 grainflow beds produced by the avalanching of dry sand as dunes migrated under the influence of northwesterly winds; and (2) wedges of wind-ripple laminae that overlie erosional surfaces produced by along-slope winds that reoriented the dune crest and moved sand obliquely up the southeast-facing slope (Fig. 2). Within packages, individual grainflow beds are separated by thin layers ('pinstripes') of finer sand deposited during short-term wind reversals (Fig. 3). Cycles in the Navajo Sandstone have been interpreted as annual increments because the distance of dune migration during a single cycle (about 1.5 m) is much too great for a day, but appropriate for a year. Longer periodicities (for example, those resulting from sunspot cycles or other multi-annual climate cycles) are highly unlikely to generate such a regular and clearly delineated record[4,9]. Furthermore, the number of grainflow-separating pinstripes in a package (20–50) is comparable to the number of wind reversals per year at selected modern meteorological stations. In the modern subtropics and middle latitudes, surface winds reverse several times per month. At In Salah, Algeria (27° N), winds above the sand-moving threshold reversed 48 times in 1988; at Niamey, Niger (13.5° N), 15 reversals were recorded in 1984[10]. These data also support an annual periodicity for Navajo Sandstone depositional cycles.

Within the lower part of the Navajo Sandstone in southern Utah and northern Arizona, synsedimentary thrust faults, folds, and breccia sheets are locally common within sets of grainflow-dominated (that is, avalanche-dominated) cross-strata (see Figs 3
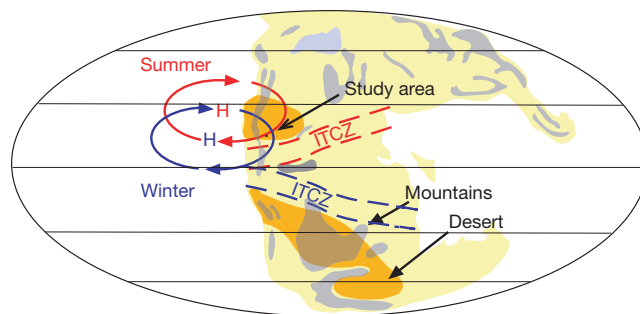

Figure 1 Pangaea during deposition of the Navajo Sandstone in the Early Jurassic. The figure shows the location of the study site (see also Supplementary Information), and the locations of deserts and mountains[1,2]. Also shown are the suggested positions of the anticyclone near the west coast of the supercontinent (H), and of the intertropical convergence zone (ITCZ); these positions are shown for the Northern Hemisphere summer (shown red) and winter (shown blue).

64   NATURE | VOL 412 | 5 JULY 2001 | www.nature.com

and 4, and Supplementary Information). The folded and faulted strata and breccia clasts consist of grainflow and wind-ripple strata that moved down the dip of the cross-strata. The upper surfaces of these disturbed zones are sharply delineated by smooth erosional surfaces that are overlain by undeformed dune deposits (see Figs 3 and 4, and Supplementary Information). These relationships indicate that deformation pre-dated cementation, and took place on the lee face of the dunes. We interpret the faults, folds, and breccia as products of the downslope movement of cohesive sediment masses. Rain-wetted blocks of cohesive sand have been observed on many modern dune slopes, and the internal structure of the coastal dunes of Brazil and Oregon[11–13] shows many features similar to those that we have observed in Jurassic outcrops. In the Navajo Sandstone, the masses of cohesive sand are isolated within a voluminous matrix of material emplaced by avalanches of dry, cohesionless sand. We infer that these two distinct types of mass movement record wet and dry conditions on the dune slope at different times.

The thrusted slabs record movement of coherent masses of dune sand, which, in a desert, would only be likely if porewater pressure were increased. In modern dunes on the Oregon coast, mass movements of cohesive sand are generated by failure of upper dune slopes that have been oversteepened by wet grainfall—a process operative when sand-driving winds are accompanied by rain[13]. However, because the Jurassic dunes were at least 33 m high[4], and because thrust faults are present in the wind-ripple deposits abutting lower dune slopes, it is improbable that the slide masses record oversteepening either by wet deposition at the top of slope or by undercutting at the toe. In an inland setting dominated by dry grainfall, the dune slope would have been saturated only during the very short time before water delivered by a heavy rainfall event drained into the dune. Avalanched sand typically has high porosity, sometimes exceeding 50% (ref. 14). Collapse of such loosely packed sand as the wetting front migrated downwards during a rainstorm could have rapidly increased the porewater pressure

along a subsurface bedding plane, triggering translational slides.

The distribution of thrust faults, folds, and breccia within annual depositional cycles enables us to determine not only the frequency of slumping events, but also their timing relative to seasonal shifts in wind direction. Although many sets of cross-strata in our field area lack disturbed sand (Fig. 2), one set (A) that records a 36-year interval of dune migration contains 24 zones of deformed strata (Fig. 5). An underlying set (B) contains 17 cycles and has 5 deformed zones. Evidence of slumping is rare in the central part of depositional cycles. If the boundary between adjacent depositional cycles is defined as the base of the wind ripple wedge (Fig. 2), then slumped
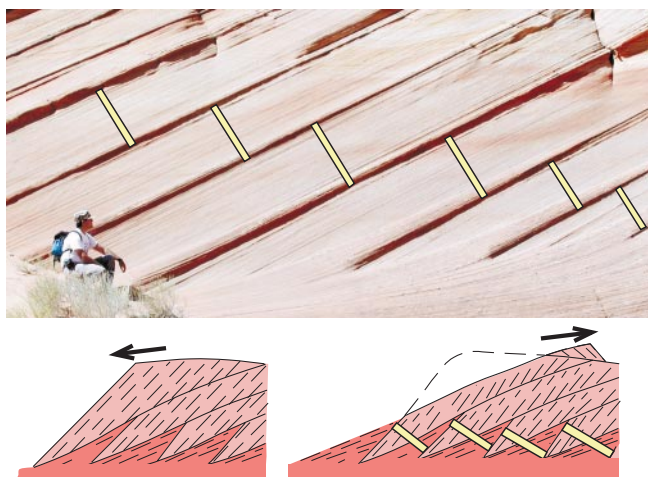

Figure 3 Parts of two successive annual depositional cycles. The cycles are shown by superimposed yellow and red bars, the positions of pinstripes (see text) are shown by white lines between grainflows, wedges of wind-rippled sand are indicated by wr, and thrust faults are arrowed. A 15-cm-thick mass of deformed sediment (red part of upper bar) lies below the erosion surface (thin red line). Rain-induced slumping followed the shift to along-slope (northeasterly) wind that deposited wind-rippled sand. Slumped sediments were buried by more wind-rippled sand before the dominant (northwesterly) wind resumed. We interpret the slumping to have taken place in summer, and the two halves of the 'split wedge' to be spring and autumn deposits. The grainflows and pinstripes, which make up more than 80% of the sediment, were deposited by the dominant winter winds.

Figure 2 Annual cycles within ancient dune cross-stratification in lower Navajo Sandstone at Coyote Buttes, Arizona. Top, wedges of wind-ripple-laminated sand extend upwards from the plinth at the base of a dune to become intercalated with packages of grainflow beds deposited by dry avalanches down the slipface of the dune, which is migrating from right to left. Undeformed yearly depositional cycles (marked by yellow columns) begin at the base of one wedge and end at the erosion surface at the base of the next wedge to the left. Bottom, schematic diagram showing the effects of the seasonal shift of northwesterly winds (bottom left) to northeasterly winds (bottom right): the dune migrates under the influence of dominant northwesterly winds as dry grainflows (light red) are deposited (bottom left), whereas the seasonal wind shift (bottom right) erodes the dune top and deposits a wedge of wind-ripple-laminated sand (dark red).
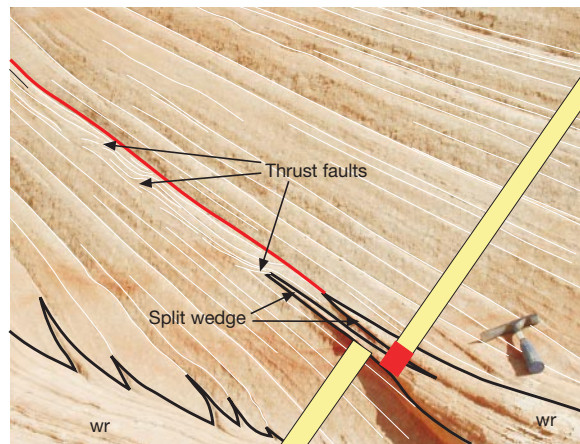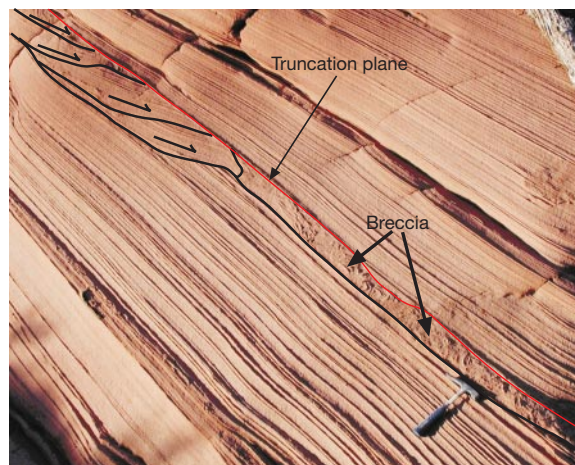

Figure 4 Slump mass and enclosing strata. The figure shows syndepositional thrust faults (arrows in upper left), and breccia that has been truncated by the erosion surface (red line) and overlain by undeformed grainflow beds. Deformation is interpreted as rain-induced slump.
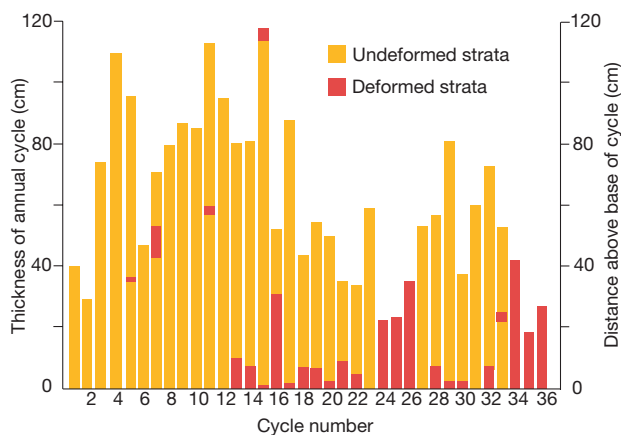
Figure 5 The properties of a continuous sequence of 36 annual cycles within 6-m-thick cross-strata of set A. Strata deformed by rain-induced slumping (red) are typically at the base or top of annual cycles, suggesting strong seasonality of major rainfall events (that is, monsoonal circulation). Thin deformed zones in mid-cycle positions (5, 7, 11 and 33) are interpreted as products of winter storms. Measured thicknesses of deformed zones were decreased by 50% to offset structural thickening. Location by Global Positioning System: 36° 55′ 49.4″ N, 112° 0′ 43.5″ W.

strata are clearly clustered at this surface. Of the 24 deformed zones in set A, 20 are bounded (above or below) by this surface. All 5 of the deformed zones in set B are in this position (see Supplementary Information). Both sets A and B are exposed in dip-parallel section. Only if all slumping were laterally continuous along the entire dune lee face would such a section intersect all slumps. Therefore, for this 36-year interval, we interpret slumping to have been an annual process.

We consider the dominant dune-driving winds to have been the northwesterly winter flow around the high-pressure zone at the western margin of Pangaea. The opposing winds that moved sand obliquely up the slip faces were the northeasterly trade winds of spring and autumn. Northeasterly flow at the southern edge of the dune field was followed by the arrival of heavy rains at the northern margin of the intertropical convergence zone (ITCZ). Slumps generated during these rains would have been truncated and buried by wind-ripple deposits when northeasterly flow resumed as the ITCZ migrated southwards again. The dunes would have resumed their southeastward migration in winter as the anticyclone off the west coast of Pangaea migrated southwards (Fig. 1).

The thicknesses of the deformed zones in Navajo Sandstone strata record rainfall magnitudes of individual storms. The thickest deformed zone (cycle 26, set A) measures 84 cm. Assuming a doubling of thickness during thrusting, and that the slope failure was caused by positive porewater pressure, a slab of sand about 42 cm thick would need to become saturated by water. For our calculation, we assume a porosity of 50%, residual moisture (before rainfall) of another 10%, and that failure and saturation were coincident. A minimum of 170 mm of rain would be required to saturate and destabilize such a slab.

Our observations and interpretations coincide closely with results from the only quantitative Early Jurassic climate model that is currently available[3]. In particular, this model shows that for the Navajo sand sea, winter winds were stronger than summer winds. It also shows that, during the summer, monsoonal flow of moist air entered the study area from the west and delivered an average of 2 mm rainfall per day. If the precipitation fell as heavy downpours from cumulonimbus clouds, such a quantity would be sufficient to generate the slumps that we have observed in the Navajo Sandstone. □

1. Parrish, J. T., Ziegler, A. M. & Scotese, C. R. Rainfall patterns and the distribution of coals and evaporites in the Mesozoic and Cenozoic. *Palaeogeogr. Palaeoclimatol. Palaeoecol.* **40,** 67–101 (1982).
2. Kutzbach, J. E. & Gallimore, R. G. Pangaean climates: megamonsoons of the megacontinent. *J. Geophys. Res.* **94,** 3341–3357 (1989).
3. Chandler, M., Rind, D. & Ruedy, R. Pangaean climate during the Early Jurassic: GCM simulations and the sedimentary record of paleoclimate. *Bull. Geol. Soc. Am.* **104,** 543–559 (1992).
4. Kvale, E. P. *et al.* Evidence of seasonal precipitation in Pennsylvanian sediments of the Illinois basin. *Geology* **22,** 331–334 (1994).
5. Kocurek, G. & Dott, R. H. Jr in *Mesozoic Paleogeography of West-Central United States* (eds Reynolds M. W. & Dolly, E. D.) 101–116 (Rocky Mountain Section, Society of Economic Paleontologists and Mineralogists, Denver, 1983).
6. Blakey, R. C., Peterson, F. & Kocurek, G. Synthesis of late Paleozoic and Mesozoic eolian deposits of the western interior of the United States. *Sedim. Geol.* **56,** 3–125 (1988).
7. Parrish, J. T. & Peterson, F. Wind directions predicted from global circulation models and wind directions determined from eolian sandstones of the western United States. *Sedim. Geol.* **56,** 261–282 (1988).
8. Hunter, R. E. & Rubin, D. M. in *Eolian Sediments and Processes* (eds Brookfield, M. E. & Ahlbrandt, T. S.) 429–454 (Elsevier, Amsterdam, 1983).
9. Chan, M. A. & Archer, A. W. Spectral analysis of eolian foreset periodicities: implications for Jurassic decadal-scale paleoclimatic oscillators. *Paleoclimates* **3,** 239–255 (1999).
10. Loope, D. B. & Rowe, C. M. Jurassic desert storms: reactivation surfaces and wind ripple wedges that punctuate grainflow tongues within the Navajo Sandstone and record the passage of cyclonic depressions. *Geol. Soc. Am. Abstr. Progm* **32,** A308 (2000).
11. Cooke, R., Warren, A. & Goudie, A. *Desert Geomorphology* Fig. 23.22, 338 (UCL Press, London, 1993).
12. Bigarella, J. J., Becker, R. D. & Duarte, G. M. Coastal dune structures from Paran, Brazil. *Mar. Geol.* **7,** 5–55 (1969).
13. Hunter, R. E., Richmond, B. M. & Alpha, T. R. Storm-controlled oblique dunes of the Oregon Coast. *Bull. Geol. Soc. Am.* **94,** 1450–1465 (1983).
14. Hunter, R. E. Basic types of stratification in small eolian dunes. *Sedimentology* **24,** 361–387 (1977).

....

Morphological and ecological complexity in early eukaryotic ecosystems

Emmanuelle J. Javaux*, Andrew H. Knoll* & Malcolm R. Walter†

* *Botanical Museum, Harvard University, Cambridge, Massachusetts 02138, USA*
† *Australian Centre for Astrobiology, Department of Earth and Planetary Sciences, Macquarie University, New South Wales 2109, Australia*

....

Molecular phylogeny and biogeochemistry indicate that eukaryotes differentiated early in Earth history. Sequence comparisons of small-subunit ribosomal RNA genes suggest a deep evolutionary divergence of Eukarya and Archaea[1]; $C_{27}–C_{29}$ steranes (derived from sterols synthesized by eukaryotes) and strong depletion of ^{13}C (a biogeochemical signature of methanogenic Archaea) in 2,700 Myr old kerogens independently place a minimum age on this split[2,3]. Steranes, large spheroidal microfossils, and rare macrofossils of possible eukaryotic origin occur in Palaeoproterozoic rocks[4–6]. Until now, however, evidence for morphological and taxonomic diversification within the domain has generally been restricted to very late Mesoproterozoic and Neoproterozoic successions[7]. Here we show that the cytoskeletal and ecological prerequisites for eukaryotic diversification were already established in eukaryotic microorganisms fossilized nearly 1,500 Myr ago in shales of the early Mesoproterozoic Roper Group in northern Australia.